13th International Symposium on Turbulence and Shear Flow Phenomena (TSFP13)
Montreal, Canada, June 25–28, 2024

DEVELOPMENT OF FEEDBACK CONTROL LAW FOR WALL TURBULENCE BY COMBINING OPTIMAL CONTROL THEORY AND BAYESIAN OPTIMIZATION

Yusuke Yugeta
Department of Mechanical Engineering
The University of Tokyo
7-3-1 Hongo, Bunkyo-Ku, Tokyo 113-8656, Japan
ygt0225@iis.u-tokyo.ac.jp

Yosuke Hasegawa
Institute of Industrial Science
The University of Tokyo
4-6-1 Komaba, Meguro-ku, Tokyo 153-8505, Japan
ysk@iis.u-tokyo.ac.jp

ABSTRACT

In the last few decades, optimal control theory has been successfully applied to wall turbulence, and remarkable control performances have been reported. Meanwhile, the resulting performances are highly dependent on a cost function to be minimized, and its selection has been made based on numerious trials and errors based upon researchers' insight. In this study, we define the cost function as a linear sum of quadratic terms of various wall quantities, and their weight coefficients are optimized to maximize the resulting drag reduction rate. It is shown that the fluctuation of the spanwise wall shear stress has a large impact on the drag reduction rate obtained in the suboptimal control as reported in Lee *et al.* (1998), while non-negligible contributions to skin friction drag from other wall quantities are also identified. As a result, the newly propsoed cost function improves the control performance from those reported in existing studies.

INTRODUCTION

Wall turbulence can be found in various thermo-fluids systems and its prediction and control are of fundamental importance in engineering. However, the non-linear and multi-scale nature of wall turbulence makes it challenging to develop accurate prediction models and effective control methods (Brunton & Noack, 2015).

Among various control schemes developed so far, adjoint-based optimal control (Abergel & Temam, 1990; Bewley *et al.*, 2001) has resulted in significant control performances by explicitly considering the mathematical models of fluid flow in deriving the control inputs. Specifically, the laminarization of a fully developed channel flow at a low Reynolds number was achieved by applying the optimal control input (Bewley *et al.*, 2001) with a far smaller magnitude than those of the other types of control inputs achieving relaminarization such as a traveling wave of wall blowing and suction Min *et al.* (2006). One of the drawbacks of the optimal control theory is that it requires the iterations of forward and adjoint analyses, and this becomes an obstacle to applying it to online control in an experiment. The suboptimal control is a kind of optimal control, where the time horizon is assumed to be vanishingly small. This allows one to derive the suboptimal control input analytically without conducting the expensive forward-adjoint looping. According to Lee *et al.* (1998), a significant drag reduction effect can be still achieved by setting the cost function as the fluctuation of the spanwise wall shear stress. However, it is important to note that, in their control, the algorithm aims at enhancing the spanwise wall shear stress fluctuation in a subsequent time step, while the spanwise wall shear stress eventually decays by continously applying the control for a long period, and the streamwise mean wall shear stress is also reduced. This indicates that the relationship between a short-term control target, i.e., a cost function, and the resulting drag reduction rate is not trivial, and even a higher control performance could be achieved by setting an appropriate cost function. However, no attempt to systematically optimize the cost function have been reported so far.

In the present study, we aim to find effective wall quantities to be included in the cost function in the framework of the suboptimal theory for reducing the skin friction drag in a fully developed turbulent channel flow. The cost function is expressed by a linear sum of various wall quantities and their weight coefficients are optimized by Bayesian optimization to maximize the resulting drag reduction rate. Based on the obtained results, we will discuss how each short-term control target is related to the long-term drag control effect.

PROBLEM AND NUMERICAL SETUPS

In this study, we perform direct numerical simulations (DNSs) of a fully developed turbulent channel flow as schematically shown in Fig. 1 under a constant flow rate condition. The bulk Reynolds number is set to be $\mathrm{Re}_b = 2U_b h/\nu = 3220$, where U_b, h, and ν are the bulk mean velocity, the channel-half height, and the kinematic viscosity of the fluid, respectively. This flow configuration corresponds to the friction Reynolds number of $\mathrm{Re}_\tau = u_\tau h/\nu \approx 110$ in the uncontrolled flow, where u_τ is a friction velocity. The fluid is assumed to be incompressible and Newtonian, and the corresponding governing equations are the following continuity and Navier-Stokes equations which are solved by using the open-source solver Incompact3d (Laizet & Lamballais, 2009; Laizet & Li, 2011):

$$\frac{\partial u_i}{\partial t} + \frac{\partial (u_i u_j)}{\partial x_j} = -\frac{\partial p}{\partial x_i} + \frac{1}{\mathrm{Re}_b}\frac{\partial^2 u_i}{\partial u_j \partial u_j}, \tag{1}$$

$$\frac{\partial u_i}{\partial x_i} = 0. \tag{2}$$

The streamwise, wall-normal and spanwise coordinates are denoted by (x,y,z), while the corresponding velocity components are (u,v,w). Periodic boundary conditions are imposed in the x and z directions, whereas no-slip boundary conditions are adopted for u and w on the top and bottom walls. The wall boundary condition for v is determined based on the suboptimal control in the controlled flow, while it is also set to be null for the uncontrolled flow. Throughout this study, all the variables are normalized by U_b and h. The dimension of the computational domain is $L_x \times L_y \times L_z = 4\pi \times 2 \times 4/3\pi$ with computational grids of $N_x \times N_y \times N_z = 128 \times 129 \times 96$. The computations were performed using the Cartesian coordinate system with uniform grid spacings in the streamwise and spanwise directions, and the grid becoming finer with approaching the walls, as proposed by Laizet & Lamballais (2009). The grid resolution in each direction is $(\Delta x^+, \Delta y^+, \Delta z^+, \Delta t^+) = (10.7, 0.6-4.8, 4.8, 0.02)$, where the superscript of $+$ represents a value in the wall-unit of the uncontrolled flow.

SUBOPTIMAL CONTROL

We define the cost function as

$$\begin{aligned} J \equiv \Bigg\langle \phi^2 + a_1 \frac{\partial u}{\partial y}^2 + a_2 \frac{\partial u}{\partial y}\frac{\partial w}{\partial y} + a_3 \frac{\partial u}{\partial y}\frac{\partial p}{\partial x} + a_4 \frac{\partial u}{\partial y}\frac{\partial p}{\partial z} \\ + a_5 \frac{\partial w}{\partial y}^2 + a_6 \frac{\partial w}{\partial y}\frac{\partial p}{\partial x} + a_7 \frac{\partial w}{\partial y}\frac{\partial p}{\partial z} + a_8 \frac{\partial p}{\partial x}^2 \\ + a_9 \frac{\partial p}{\partial x}\frac{\partial p}{\partial z} + a_{10} \frac{\partial p}{\partial z}^2 \Bigg\rangle. \end{aligned} \tag{3}$$

The cost functions described previously are applicable solely to the lower wall of the system. Conversely, the cost functions for the upper wall have been appropriately modified to account for the inherent symmetry of the overall system. Here, p is the static pressure, and the parenthesis $\langle\cdot\rangle$ represents the surface integral over the top and bottom walls. Accordingly, the present cost function includes only wall quantities. The weight coefficients a_i $(i = 1-10)$ will be optimized by Bayesian optimization as explained later. Once the cost function (3) is defined, the suboptimal control input can be analytically derived by using the instantaneous flow information following the essentially same procedures reported in (Lee *et al.*, 1998). Note that the cost function (3) can be considered as a general form of those proposed in Lee *et al.* (1998) which correspond to the cases with $a_1 > 0$ and $a_i = 0$ $(i \neq 1)$, and $a_5 < 0$ and $a_i = 0$ $(i \neq 5)$ in the present study. We also note that the derived suboptimal control input is normalized, so that its root-mean-square value becomes $\phi^+_{\mathrm{RMS}} = v^+_{\mathrm{RMS}}(y^+ = 10)$ at each time step. Furthermore, although not explicitly stated in Eq. (3), each term ($\partial w/\partial y|^2$, $\partial u/\partial y \partial p/\partial x$ etc.) is normalized to be unit with the value at the onset of the control. Therefore, only the ratios among the weight coefficients a_i are important, while their magnitudes do not affect the control input.

BAYESIAN OPTIMIZATION

As the optimization tool, we employed Bayesian optimization, with which one can effectively find the optimum design parameters with a small number of trials in a probabilistic manner. In the present study, the Bayesian optimization framework is implemented via the open-source Python library Optuna with Tree-structured Parzen Estimator as a surrogate function.

The coefficients a_i in the cost function (3) are optimized so as to minimize the time-averaged $C_f \equiv \tau_w/(1/2\rho U_b^2)$ value within $t^+ \in [600, 1200]$, where $t^+ = 0$ indicates the onset of the control. Depending on the cost function, the computation becomes unstable and eventually diverges. In such a case, we set a large value to C_f, i.e., unity in the present study, for penalization. The weight coefficients are updated at the onset of the control and kept constant throughout each trial starting from the same initial condition. The diagram in Fig. 2 outlines the steps involved in the current framework.

In the present study, the Bayesian optimization framework is implemented via the open-source Python library Optuna Akiba *et al.* (2019), with Tree-structured Parzen Estimator Bergstra *et al.* (2011) as a surrogate function. The readers are reffered to the literature for details.

RESULTS AND DISCUSSIONS

Figure 3 shows the obtained C_f with the trial number. Although about 50 trials have yielded drag reduction rates that exceed that of Lee *et al.* (1998), the optimization is further continued to ensure that it is converged. After 150 trials, we obtain the lowest value of C_f around 6.5×10^{-3}, which is slightly lower than C_f achieved with the existing cost functions.

The weight coefficients in the five successful cases with the highest drag reduction rates are shown in Fig. 4. First, concerning the weight of $\partial w/\partial y|^2$, the top five trials all have large negative values, consistent with the results of Lee *et al.* (1998) where the control tries to maximize the spanwise shear at each time step. Also, the resultant drag reduction rate is almost comparable to that of Lee *et al.* (1998).

Meanwhile, we note that the weights for other terms besides $\partial w/\partial y|^2$ are non-zero, indicating that they would also affect the control performance. For instance, the weights for $\partial p/\partial x|^2$ and $\partial p/\partial x \partial p/\partial z$ have large positive values, and the effectiveness of these terms are newly identified in the present study. These terms may contribute to stabilize streaky structures (Koumoutsakos, 1999; Endo & Kasagi, 2001). In addition, the weight coefficient for $\partial p/\partial z^2$ is given a negligible value, while the sole use of this term as a cost function is reported to be effective by Lee *et al.* (1998) and also confirmed by our pilot study.

In order to clarify the sensitivity of each weight coefficient to the resulting drag reduction rate, the FANOVA importance(Hutter *et al.*, 2014) of each term is evaluated and the results are shown in Fig. 5. These results indicate that the present successful cost functions commonly have negative weight coeffficents for $\partial w/\partial y|^2$, and this agrees with that proposed by Lee *et al.* (1998), where it is demonstrated that applying a control input so as to enhance the fluctuation of the spanwise wall shear stress in a short term is effect in reducing the skin friction drag in a long-term perspective. Even though our exploration space is still limited to the prescribed library, our result is consistent with numerous literature (Choi *et al.*, 1994; Lee *et al.*, 1998) in the point that linear cancellation of streamwise vortex structures provides an effective control law when only using short-period information.

Finally, the instantaneous distribution of the streamwise velocity component, the applied control input, and quasi-streamwise vortex structures are visualized in Fig. 6 with the best weights from the optimization.The current control algorithm is observed to apply robust blowing and suction near the vortical structures, akin to the opposition control approach described by Choi *et al.* (1994). However, the algorithm is capable of handling each flow scale independently. Additionally, the structure of the control input appears to be tilted at an angle relative to the primary flow direction, which represents a subtle difference compared to the approach proposed by Lee *et al.* (1998).

CONCLUSION

The optimal control theory has been successfully applied to determine the spatio-temporal distribtuion of a control input for turbulence control. Meanwhile, it requires to specify a cost function to be minimized, and it has conventionally been made by researchers' insights. The present study aimed to systematically optimize a cost function in order to obtain novel control strategies leading to better control performances. Specifically, within the framework of the suboptimal control, the cost function was formulated as a weighted sum of squared wall quantities such as wall shear stress and wall pressure, and the weighting coefficients were optimized using the Bayesian optimization. The results showed that, in addition to the term related to the spanwise wall shear stress reported to be effective in previous studies, the optimal weighting coefficients indicates including other novel terms in the cost function also contributes to considerable drag reduction. Although the present study considers the control of a canonical flow, the proposed framework can be easily extended to more complex flow configurations, and therefore is expected to yield novel flow control strategies and achieve higher control performances.

REFERENCES

Abergel, F. & Temam, R. 1990 On some control problems in fluid mechanics. *Theoretical and Computational Fluid Dynamics* **1** (6), 303–325.

Akiba, Takuya, Sano, Shotaro, Yanase, Toshihiko, Ohta, Takeru & Koyama, Masanori 2019 Optuna: A Next-generation Hyperparameter Optimization Framework. In *Proceedings of the 25th ACM SIGKDD International Conference on Knowledge Discovery & Data Mining*, pp. 2623–2631. New York, NY, USA: Association for Computing Machinery.

Bergstra, James, Bardenet, Rémi, Bengio, Yoshua & Kégl, Balázs 2011 Algorithms for Hyper-Parameter Optimization. In *Advances in Neural Information Processing Systems*, , vol. 24. Curran Associates, Inc.

Bewley, Thomas R., Moin, Parviz & Temam, Roger 2001 DNS-based predictive control of turbulence: an optimal benchmark for feedback algorithms. *Journal of Fluid Mechanics* **447**, 179–225.

Brunton, Steven L. & Noack, Bernd R. 2015 Closed-loop turbulence control: Progress and challenges. *Applied Mechanics Reviews* **67** (5), publisher: American Society of Mechanical Engineers (ASME).

Choi, Haecheon, Moin, Parviz & Kim, John 1994 Active turbulence control for drag reduction in wall-bounded flows. *Journal of Fluid Mechanics* **262**, 75–110, publisher: Cambridge University Press.

Endo, Takahide & Kasagi, Nobuhide 2001 Active Control of Wall Turbulence with Wall Deformation. *JSME International Journal Series B Fluids and Thermal Engineering* **44** (2), 195–203.

Hutter, Frank, Hoos, Holger & Leyton-Brown, Kevin 2014 An efficient approach for assessing hyperparameter importance. In *Proceedings of the 31st International Conference on International Conference on Machine Learning - Volume 32*, pp. I–754–I–762. Beijing, China: JMLR.org.

Koumoutsakos, Petros 1999 Vorticity flux control for a turbulent channel flow. *Physics of Fluids* **11** (2), 248–250.

Laizet, Sylvain & Lamballais, Eric 2009 High-order compact schemes for incompressible flows: A simple and efficient method with quasi-spectral accuracy. *Journal of Computational Physics* **228** (16), 5989–6015.

Laizet, Sylvain & Li, Ning 2011 Incompact3d: A powerful tool to tackle turbulence problems with up to O(105) computational cores. *International Journal for Numerical Methods in Fluids* **67** (11), 1735–1757, _eprint: https://onlinelibrary.wiley.com/doi/pdf/10.1002/fld.2480.

Lee, Changhoon, Kim, John & Choi, Haecheon 1998 Suboptimal control of turbulent channel flow for drag reduction. *Journal of Fluid Mechanics* **358**, 245–258.

Min, Taegee, Kang, Sung Moon, Speyer, Jason L. & Kim, John 2006 Sustained sub-laminar drag in a fully developed channel flow. *Journal of Fluid Mechanics* **558**, 309–318.

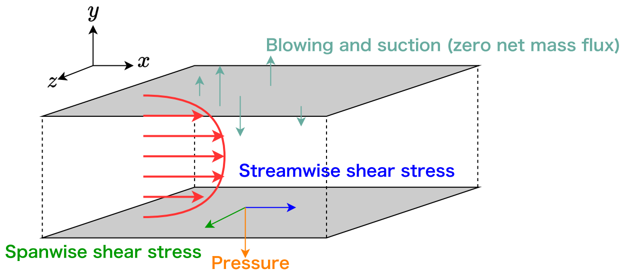

Figure 1. Flow configuration and coordinate system in the present study

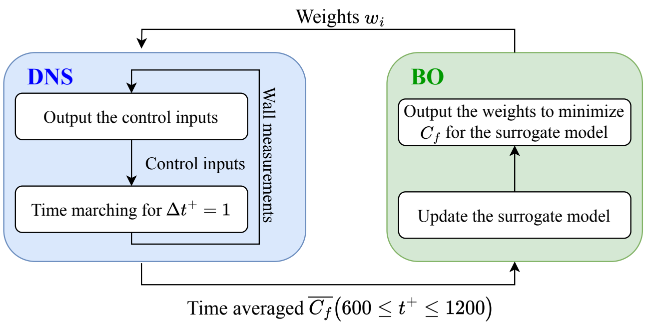

Figure 2. Flowchart of the present optimization framework. The left blue box is a process of direct numerical simulation, whereas the right green box is a process of Bayesian optimization.

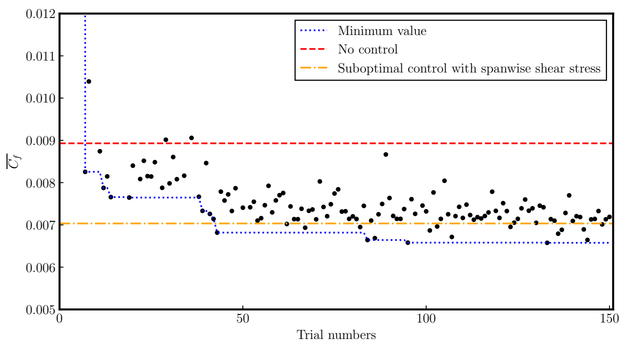

Figure 3. Time averaged friction coefficient $\overline{C_f}$ from $t^+ = 600$ to 1200 in the optimization process of Case 2; each black dots indicates each trials; blue dotted line indicates the elite case so far; red dash line indicates uncontrolled case; yellow dash-dot line indicates the original suboptimal control Lee *et al.* (1998) with spanwise shear stress.

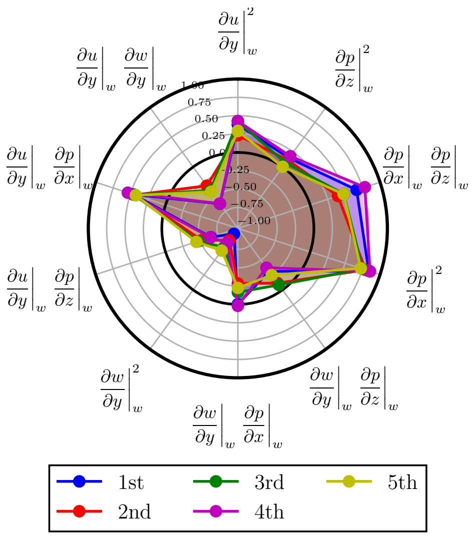

Figure 4. Weights parameter distribution for the top 5 drag-reducing cases. Blue: the most reduced, Red: the 2nd, Green: the 3rd; Purple: the 4th, and Yellow: the 5th. The closer the circle is to the center, the closer the weight is to -1, and the further out it is, the closer the weight is to 1. The concentric circle in bold lines indicates the weight to be zero.

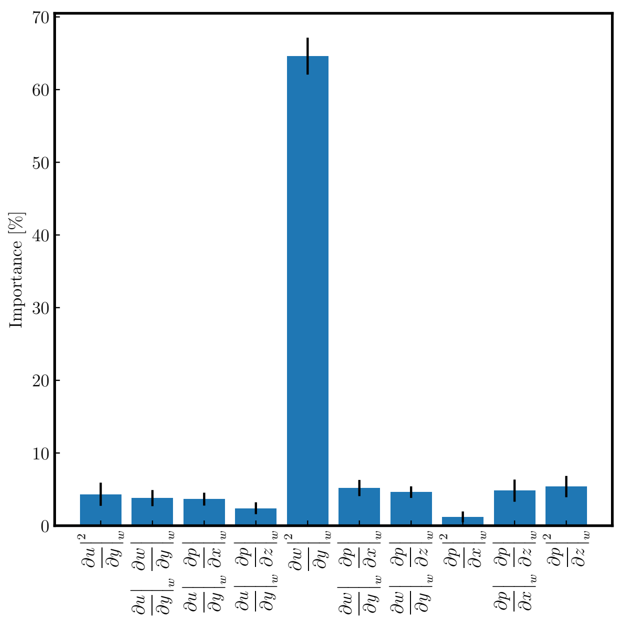

Figure 5. fANOVA importance (Hutter *et al.*, 2014) among the present weights to be optimized in Case 2; The values show how much importance is given to the weight parameters in relation to the metrics.; The vertical black lines indicate their standard deviation through ten computations.

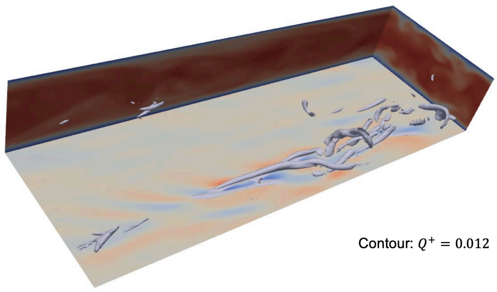

Figure 6. Instantaneous flow visualization for the best cost function. The side walls show streamwise velocity, while the bottom wall shows the wall-normal velocity (control inputs). The three-dimensional contour shows the iso-surface of the second-invariant of the velocity gradient tensor.